Optofluidic characterization of marine algae using a microflow cytometer

Nastaran Hashemi, Jeffrey S. Erickson, Joel P. Golden, and Frances S. Ligler

Citation: Biomicrofluidics **5**, 032009 (2011); doi: 10.1063/1.3608136
View online: http://dx.doi.org/10.1063/1.3608136
View Table of Contents: http://bmf.aip.org/resource/1/BIOMGB/v5/i3
Published by the AIP Publishing LLC.

Optofluidic characterization of marine algae using a microflow cytometer

Nastaran Hashemi, Jeffrey S. Erickson, Joel P. Golden, and Frances S. Ligler[a)]
Center for Bio/Molecular Science and Engineering, Naval Research Laboratory, Washington, DC, USA

(Received 18 March 2011; accepted 3 May 2011; published online 20 September 2011)

The effects of global warming, pollution in river effluents, and changing ocean currents can be studied by characterizing variations in phytoplankton populations. We demonstrate the design and fabrication of a Microflow Cytometer for characterization of phytoplankton. Guided by chevron-shaped grooves on the top and bottom of a microfluidic channel, two symmetric sheath streams wrap around a central sample stream and hydrodynamically focus it in the center of the channel. The lasers are carefully chosen to provide excitation light close to the maximum absorbance wavelengths for the intrinsic fluorophores chlorophyll and phycoerythrin, and the excitation light is coupled to the flow cytometer through the use of an optical fiber. Fluorescence and light scatter are collected using two multimode optical fibers placed at 90-degree angles with respect to the excitation fiber. Light emerging from these collection fibers is directed through optical bandpass filters into photomultiplier tubes. The cytometer measured the optical and side scatter properties of *Karenia b*., *Synechococcus* sp., *Pseudo-Nitzchia*, and *Alexandrium*. The effect of the sheath-to-sample flow-rate ratio on the light scatter and fluorescence of these marine microorganisms was investigated. Reducing the sample flow rate from 200 μL/min to 10 μL/min produced a more tightly focused sample stream and less heterogeneous signals. © *2011 American Institute of Physics*. [doi:10.1063/1.3608136]

I. INTRODUCTION

Due to global and local environmental concerns, a substantial need exists for real-time characterization of quickly changing ocean conditions and alterations in marine life.[1] Pollution and environmental change can cause significant variation in populations of phytoplankton species. Generally, phytoplankton species are collected and later analyzed onshore in marine laboratories. However, real-time analysis of phytoplankton has been a matter of great interest among marine biologists. Flow cytometry has been employed to investigate marine microorganisms and the changes in their population.[2] The CytoBuoy and FlowCytobot are successful examples of marine flow cytometers.[3] However, these flow cytometers have the following limitations: high manufacturing cost, large size, and significant power requirements. A more readily deployable cytometer that could tolerate high pressure, occupy a very small footprint, and require minimal power would be of significant benefit.

Over the last decade, researchers have focused on using microfluidics to create flow cytometers with very small footprints. One of the unique requirements for a flow cytometer to characterize marine algae is that it must accommodate particles over a wide size range (ideally 1 micron up to hundreds of microns). Many microflow cytometers focus the sample stream only on the sides prior to laser interrogation of the particles. Thus, the confinement of the stream in the vertical direction to align cells in the laser beam must rely on using very small channel heights, and such channels cannot accommodate the larger algae. Therefore, microfluidic cytometers that perform three-dimensional (3D) hydrodynamic focusing of the sample

[a)]Author to whom correspondence should be addressed. Electronic mail: Frances.ligler@nrl.navy.mil. Tel.: 202-404-6002.

stream would be beneficial for marine analysis. Shoji *et al.*[4] introduced one of the first coaxial focusing techniques using a smaller sample inlet and a two-step introduction of carrier flows. Later, Wolff *et al.*[5] presented a chimney-like structure and Sundararajan *et al.*[6] fabricated a chip using the sandwich method to create coaxial sheathing. Sato *et al.*[7] presented a design that used grooves to bring sheath fluid from the side of the channel compressing the sample stream downward to the center of the microchannel, but the sample stream was substantially distorted. Mao *et al.*[8] introduced the "microfluidic drifting" technique: the sample stream was drifted due to the transverse secondary flow induced by the centrifugal effect in the curve of a microchannel, and then it was compressed vertically from both sides using two horizontal focusing sheath flows. Hairer *et al.*[9] presented a hydrodynamic focusing device that ensheathed the sample stream using a tapered section, a lifting sheath inlet, and side sheath ports. The sample fluid was introduced into the channel vertically. None of these approaches for 3D focusing of the sample stream are sufficiently simple for incorporation into an underwater flow cytometer.

We designed a much simpler microfluidic device for 3D focusing of the sample stream and are integrating it into a miniaturized microflow cytometer to study marine phytoplankton. Guided by chevron-shaped grooves on the top and bottom of a microchannel, the sheath fluid focuses the sample stream into the center of the channel. Relative flow rates of the sheath and sample fluids can be used to control the width of the focused sample stream in the interrogation region. Optical excitation of individual phytoplankton passing through the interrogation region produces the light scatter and fluorescence signals. The resolution of this device for discriminating three different populations of phytoplankton has been demonstrated using a 488 nm argon laser for direct comparison to a commercial benchtop cytometer.[10] Reversing the hydrodynamic focusing was also demonstrated as a means to recycling the sheath fluid for long-term unattended operation if that becomes an important factor for underwater utility.[11] Traditionally, 488 nm lasers are argon-ion gas lasers. They are large, require cooling, and are power intensive. In this paper, 404 nm and 532 nm diode lasers provide excitation for chlorophyll a and phycoerythrin closer to their maximum excitation wavelengths than was provided by the 488 nm laser. The lasers themselves are also more appropriate for underwater applications. We have also studied the effect of sheath-to-sample flow rate ratios on the mean and coefficient of variations (CVs) of light scatter, chlorophyll fluorescence, and phycoerythrin fluorescence data for four different phytoplankton species.

II. EXPERIMENTAL DETAILS

A. Microfluidic design

The sheath stream, input from a single reservoir, was split and introduced into the microflow cytometer on either side of the sample stream. This configuration positioned the sample stream in the center of the channel horizontally and minimized the impact of pulses from the peristaltic pump on the lateral position of the sample stream. Chevrons molded into the top and bottom of the channel directed the sheath fluid from the sides of the channel toward the top and bottom and compressed the sample stream vertically. The number of chevrons controls the height of the sample stream in the focused region and the flow-rate ratio of sample and sheath flows determines the width.[11,12] The dimensions of the polydimethylsiloxane (PDMS) microchannel were 390 μm wide by 130 μm deep. A relatively large sample inlet width of 390 μm minimized destruction of larger phytoplankton species. The chevron-shaped grooves were 100 μm wide by 65 μm deep and intersected the channel wall at 45 degrees. Figure 1 shows a schematic of the experimental setup. A syringe pump (CAVRO XE 1000, Tecan Systems, Inc., San Jose, CA) and a bidirectional peristaltic pump (P625/66.143, Instech Laboratories, Inc., Plymouth, PA) were used to introduce the sample and sheath fluids into the microchannel. Details of the fabrication methods have been described elsewhere.[11,13]

B. Optical detection system

The hydrodynamic positioning, along with control of the relative flow rates of the sheath and sample streams, focused the sample stream as it crossed the laser beams in the interrogation

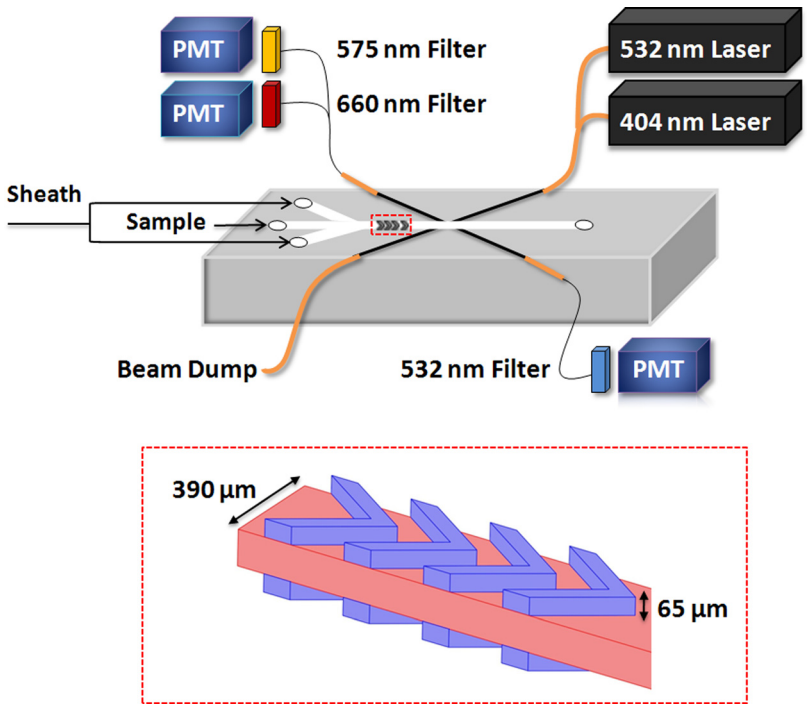

FIG. 1. A schematic of the microflow cytometer. (a) The optical and microfluidics setup. (b) A zoom-in view showing the chevron grooves extending into the PDMS substrate.

region to generate two-color fluorescence and light scatter signals. Optical excitation at 404 nm (Z80M18H-F-404-PE, 80 mW, Z-Laser Optoelektronik GmbH, Germany) and 532 nm (Z40M18B-F-532-PZ, 40 mW, Z-Laser Optoelektronik GmbH, Germany) was provided by diode and diode-pumped solid-state (DPSS) lasers, respectively (Figure 1). For excitation, a custom wavelength division multiplexing (WDM) fiber optic coupler (PSK-000797, Gould Technology LLC, Millersville, MD) was used to launch the light from both lasers into a single-mode optical fiber with a numerical aperture of 0.14. Fluorescence and light scatter were collected using multimode optical fibers with numerical apertures of 0.275. Optical fibers were cleaved and inserted into guide channels fabricated in the PDMS channel for alignment with the interrogation region. The multimode fibers were aligned at 90-degree angles with respect to the excitation fiber and directed the light using fiber splitters to photomultiplier tubes (PMTs, H9307-02, Hamamatsu, Bridgewater, NJ). A beam-dump fiber was positioned directly across the channel from the excitation fiber to reduce background from scattered excitation light. Each PMT was equipped with a bandpass filter. A 532 ± 10 nm filter (Omega Optical, Inc., Brattleboro, VT) was used for light scatter detection. As suggested in the literature,[14,15] we defined the fluorescence emission windows in the orange and red regions of the spectrum to quantify intrinsic fluorescence of phycoerythrin and chlorophyll, respectively. For convenience, we refer to the fluorescence signals in the above-mentioned windows as phycoerythrin and chlorophyll, respectively, although other chromophores could also contribute to the signal. Red fluorescence (chlorophyll) emissions and orange fluorescence (phycoerythrin) emissions were detected using 660 ± 15 nm and 575 ± 20 nm bandpass filters (Omega Optical, Inc., Brattleboro, VT). The output voltage collected from the PMTs was recorded by a 16-bit A/D board (Data Translation, Inc.) and transferred to a personal computer using a USB cable. Data from the PMTs was acquired at 200 kSPS.

C. Marine phytoplankton

The algal cultures were obtained from the National Oceanic and Atmospheric Administration (Charleston, SC). The phytoplanktonic species used for this work were *Synechococcus* sp.,

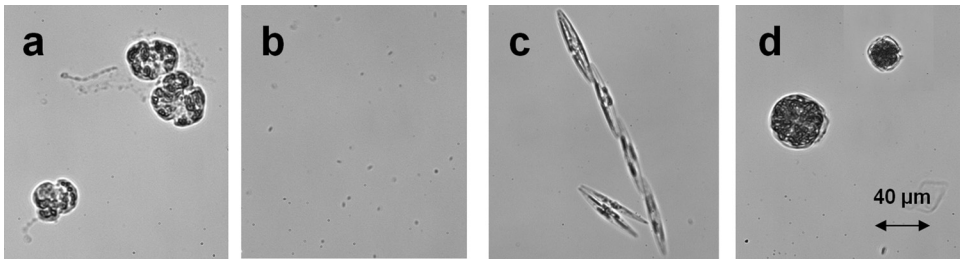

FIG. 2. Microscopy of the phytoplankton species. The photos show images of (a) *Karenia b*., (b) *Synechococcus* sp., (c) *Pseudo-Nitzchia*, and (d) *Alexandrium*.

Karenia brevis, *Alexandrium*, and *Pseudo-Nitzchia*. *Synechococcus* sp. (Cyanophyceae) is a unicellular alga. It is spherical or ellipsoidal in shape and moves by oscillating. Its reported photosynthetic pigments are chlorophyll a, phycocyanin, phycoerythrin, and carotenoids.[16] *Karenia b*. (Dinophyceae), *Alexandrium* (Dinophyceae), and *Pseudo-Nitzchia* (Bacillariophyceae) have chlorophyll a and c, carotenoids, as well as various other accessory pigments.[17,18] *Karenia b*. is roughly spherical with an irregular surface, has two flagellae, and moves in a spinning motion. *Alexandrium* is also spherical, is covered with thin thecal plates, and has two flagella—one appearing like a belt and the other along the body. *Pseudo-Nitzchia* is a pennate diatom which is enclosed in frustules made of two valves fitted together by a girdle.[15,16,19] All algae were analyzed without fixation.

We used a Nikon Eclipse TE2000U inverted microscope to image the phytoplankton species. The cells sizes were 0.8–1.5 μm for *Synechococcus* sp., 20–40 μm for *Karenia b*., and 20–48 μm in length and 18–32 μm in width for *Alexandrium*. The *Pseudo-Nitzchia* cells were 40–85 μm long and 2–4 μm wide and frequently formed chains of 2 or more cells. Bright field photographs of each microorganism are shown in Figure 2.

III. RESULTS AND DISCUSSION

A. Computational modeling

To understand the effect of relative flow rates of the sheath and sample streams on the concentration profile of the focused stream at the interrogation region, numerical modeling of the flow was performed using the COMSOL Multiphysics finite element analysis package (COMSOL Inc., Palo Alto, CA). First, we solved the Navier-Stokes equations at steady state and then solved for the diffusive transport in the microchannel

$$\begin{aligned} -\nabla \cdot \eta(\nabla \mathbf{u} + (\nabla \mathbf{u})^{\mathbf{T}}) + \rho(\mathbf{u} \cdot \nabla)\mathbf{u} &= -\nabla p \\ \nabla \cdot \mathbf{u} &= \mathbf{0}, \end{aligned} \tag{1}$$

where η is the fluid viscosity, ρ is the density, $\mathbf{u}$ indicates the velocity, and p is the pressure. Figure 3 shows the concentration profile of the focused stream before (a, c) and after (b, d) the chevron grooves. The darkest color (brown) indicates a concentration of 0 and the lightest color (white) represents a concentration of 1 in the simulations. Concentrations between these two values are shown in intermediate colors. While the sheath flow rate is held constant at 800 μL/min, the core flow rate was varied in order to investigate the effect of relative flow rates on the size of the focused stream. The core flow rates of 200 μL/min (a, b) and 10 μL/min (c, d) resulted in relative flow rates of 1/4 and 1/80. Fluorescence intensities of the sheath stream and the undiluted dye solution were assumed to be 0 and 1, respectively. The simulation results showed that the width and height of the central part of the core were 131 μm $\times$ 38 μm for the core flow rate of 200 μL/min. The height was 87 μm at the outer corners. For the core flow rate of 10 μL/min, the width and height of the core was 59 μm $\times$ 21 μm, with a 32 μm height at the outer corners.

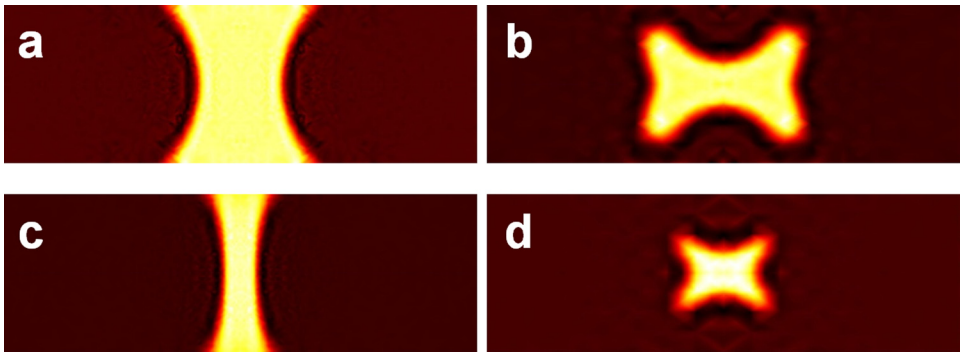

FIG. 3. Simulations showing concentration distributions of the sample stream at sheath and sample inlet flow rates of: 800 and 200 μL/min (a and b); and 800 and 10 μL/min (c and d), respectively.

B. Experimental results

The phytoplankton species were evaluated for light scatter and intrinsic fluorescence using the microflow cytometer (Figures 4–6, Table I). Data from three PMTs measured orange fluorescence (characteristic of phycoerythrin), red fluorescence (characteristic of chlorophyll), and light scatter at 532 nm. A light scatter threshold was set in the data acquisition software to trigger data collection of each phytoplankton passing through the interrogation region and to delete information from particles smaller than $\sim$1 μm. There is still likely to be some culture debris

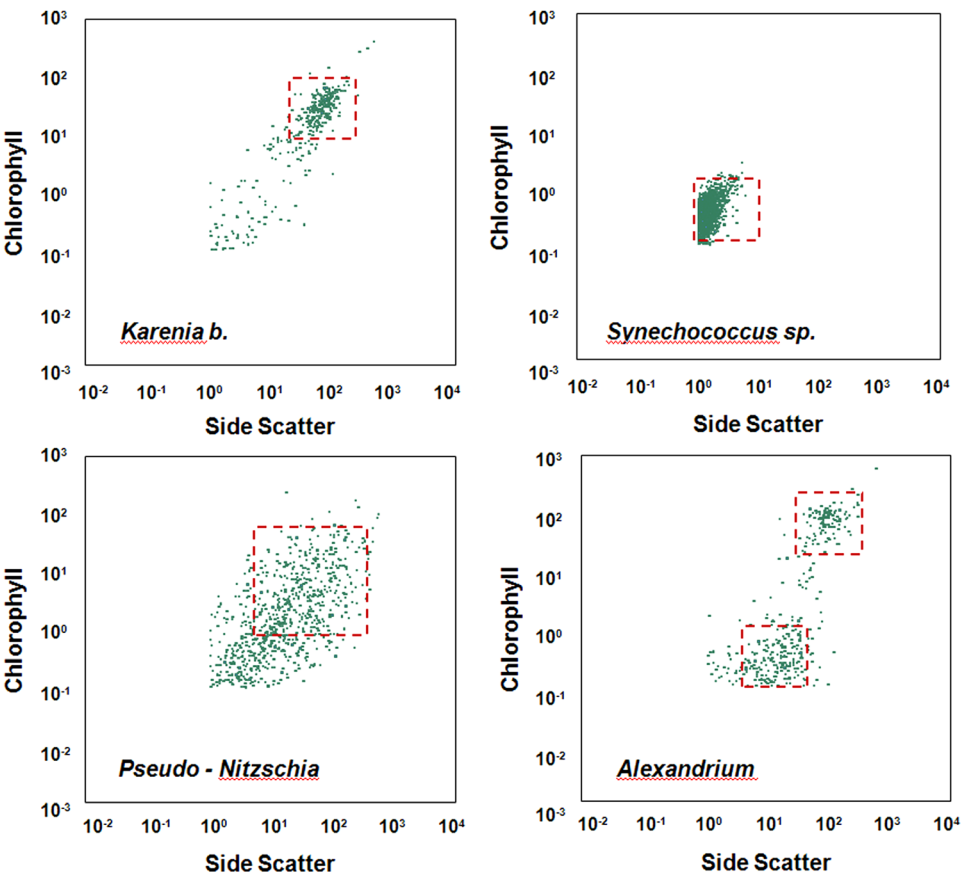

FIG. 4. Scatter plots of chlorophyll vs. side scatter signals from phytoplankton using the microflow cytometer at sheath and sample inlet flow rates of 800 and 10 μL/min. Dashed squares represent the boundaries of the cluster regions that were analyzed and described in Table II.

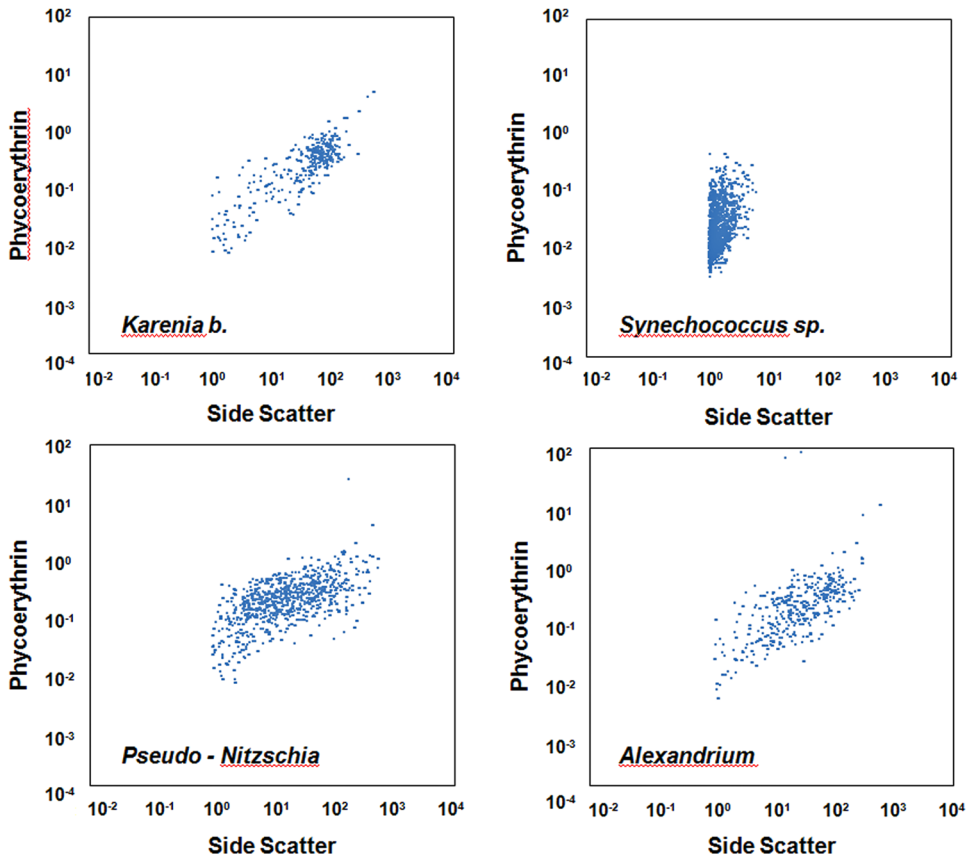

FIG. 5. Scatter plots of phycoerythryin vs. side scatter signals from phytoplankton using the microflow cytometer at sheath and sample inlet flow rates of 800 and 10 μL/min.

showing up in the scatter plots at very low light scatter levels, but we could not gate it out without decreasing the detection of the 1 μm *Synechococcus*. A chlorophyll threshold of 0.1 fluorescence units removed most of the data associated with particles with no chlorophyll fluorescence from the data set; since all of the algae tested contained chlorophyll, these particles were assumed to be from culture debris.

Chlorophyll a is strongly excited at 404 nm. A significant fluorescence signal in wavelengths longer than 650 nm was observed. Phycoerythrin was excited by the 532 nm laser and detected at 575 ± 20 nm. Figure 4 shows scatter plots depicting the magnitude of the chlorophyll fluorescence and side scatter for each cell. Both *Karenia b.* and *Alexandrium* demonstrated chlorophyll peaks at $\sim 10^2$ fluorescence units. However, *Karenia b.* showed a very small CV in comparison with *Alexandrium*, which has two significant clusters spread over the dynamic range of the PMT. Chlorophyll fluorescence was on the order of $\sim 10^{-1}$ fluorescence units for *Synechococcus* sp. and $\sim 10^1$ for *Pseudo-Nitzchia*. Phycoerythryin vs. side scatter and phycoerythryin vs. chlorophyll are shown in Figures 5 and 6, respectively. Generally, phycoerythrin fluorescence was relatively weak for all the phytoplankton studied. However, considering the small size of *Synechococcus* sp., chlorophyll is present at a higher concentration than in the larger microorganisms.

The side scatter data shows the highest values for *Pseudo-Nitzschia* and *Karenia b.* and the smallest for *Synechococcus* sp. Side scatter data are only a rough indication of the cell size and is significantly impacted by cell density, air inclusions, and other internal structures. The broadly spread scatter plot of *Pseudo-Nitzschia* could be caused either by the variable cell length and tendency to form chains (Figure 2) or by the highly elongated cells orienting at different angles to the flow to produce different scatter signals while passing through the interrogation region. Davison *et al.* have shown that non-spherical objects rotate and translate vertically

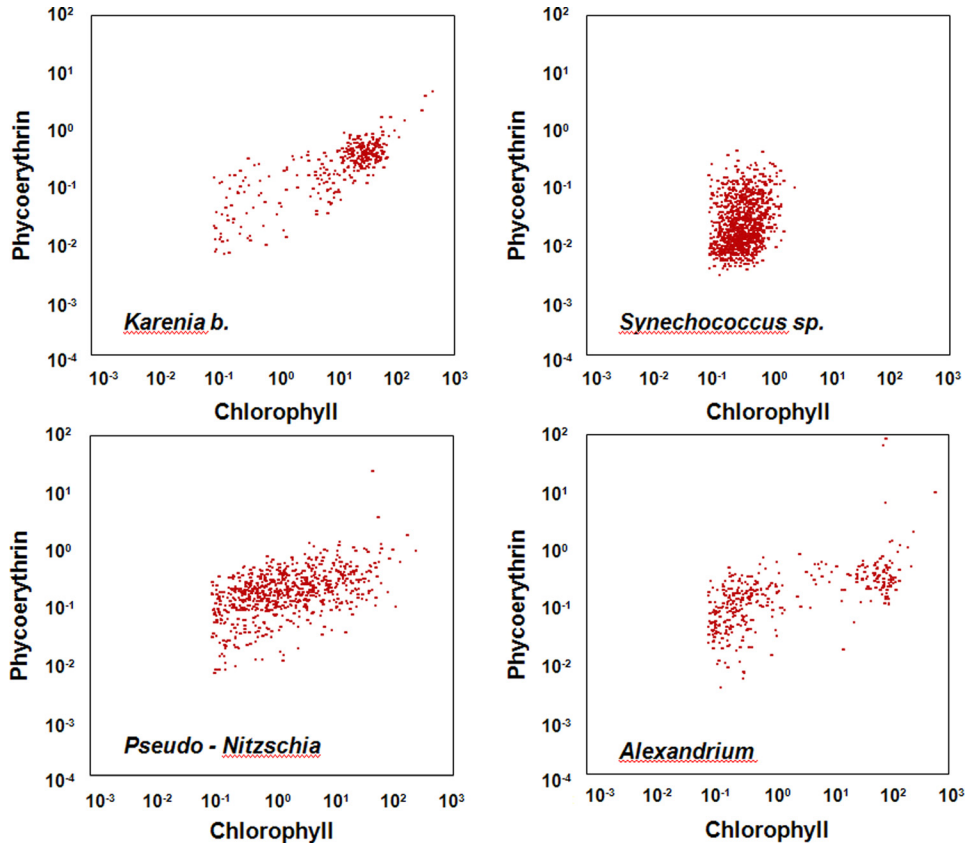

FIG. 6. Scatter plots of phycoerythryin vs. chlorophyll signals from phytoplankton using the microflow cytometer at sheath and sample inlet flow rates of 800 and 10 μL/min.

in an oscillatory pattern while in a microchannel.[20] Depending on the initial angle of the cells when they enter the channel, it is possible for the cells with the same length to pass through the interrogation region at different angles, causing different scatter signals.

The effects of the sheath-to-sample flow rate ratio on the mean and CV of light scatter, chlorophyll, and phycoerythrin signals for the four different phytoplankton species are summarized in Table I. The gates for particle inclusion were set to include particles with some level of chlorophyll and a scatter signal equal to or higher than the 1 μm *Synechococcus*. Clearly, some of the particles included in this window were debris, but we did not want to exclude anything

Table I. Statistical analysis of data collected using the Microflow Cytometer at different sample flow rates. All particles in the data plots in Figure 4 were averaged to obtain the values below for fluorescence and side scatter (SSC).

	Mean Chl.	CV Chl. (%)	Mean PE	CV PE (%)	Mean SSC	CV SSC (%)
10 µL/min						
Synechococcus sp.	0.4	63	0.03	120	1.6	41
Pseudo-Nitzschia	9.2	170	0.17	89	56.8	80
Alexandrium	26.6	190	0.66	850	49.2	120
Karenia b.	26.9	130	0.35	110	54.1	89
200 µL/min						
Synechococcus sp.	0.8	200	0.08	370	1.3	110
Pseudo-Nitzschia	6.9	240	0.28	330	41.7	160
Alexandrium	2.1	500	0.74	830	19.9	170
Karenia b.	5.9	490	0.34	970	11.9	310

Table II. Cluster analysis of data at sample flow rate of 10 μL/min. The populations analyzed are indicated in Figure 4 (dashed boxes), including the two distinct populations of *Alexandrium* indicated by g.1 and g.2.

	Mean Chl.	CV Chl. (%)	Mean PE	CV PE (%)	Mean SSC	CV SSC (%)	Mean PE/Ch
10 μL/min							
Synechococcus sp.	0.41	43	0.03	129	1.54	34	0.079
Pseudo-Nitzschia	9.21	85	0.20	69	65.6	89	0.021
Alexandrium (g.1)	81.8	34	0.34	64	110.9	44	0.004
Alexandrium (g.2)	0.62	51	0.18	68	24.3	41	0.283
Karenia b.	34.4	38	0.43	44	71.6	32	0.012

on the first analysis that might show up in a mixed population. Statistical analysis of the data (Table I) showed that CVs were much larger when the sample flow rate was 200 μL/min. This observation is consistent with the simulation results showing a larger core diameter at the flow rate of 200 μL/min.

The beam intensity across the flow stream is of Gaussian shape and diverges according to the numerical aperture of the waveguide. By hydrodynamically focusing the sample stream in a more confined region, the cells received more uniform beam intensity. If the position of the cell varies from the center of the Gaussian beam by 0.67 standard deviations, the cells received only 78% of the maximum intensity compared to a same cell that is in the center of the sample stream.[21] All of the algal populations analyzed exhibited an expected level of heterogeneity. Nonetheless, Table I indicates that a much higher variability in the signals was obtained when the cells were introduced at 200 μL/min than when they were introduced at 10 μL/min. Since the smaller core generated at the slower flow rate more tightly confined the cells in the excitation beam, the signals exhibited less variation, and the CVs were significantly reduced.

Clusters were observed in the scattergrams of Figure 4. Areas were delineated by the dashed boxes to define approximate boundaries of the clusters. Data from points inside the bounded regions of the scatter vs chlorophyll fluorescence plots were analyzed for these parameters and phycoerythrin fluorescence and the data presented in Table II. Since *Alexandrium* showed two distinct subpopulations, which could be associated with different sizes of the cells (See Figure 2), we have presented data from the separate clusters of *Alexandrium* cells in Table II. The phycoerythrin/chlorophyll ratio (PE/Chl.),[18] calculated based on the ratio of phycoerythrin to chlorophyll for each individual cell, was found to be the smallest for population g.1 in *Alexandrium* and the largest for population g.2 in *Alexandrium*. The different PE/Chl. ratios suggested the presence of different relative amounts of pigments in the two *Alexandrium* populations. Furthermore, the mean values for chlorophyll and light scatter for each of the five clusters varied widely. The phycoerythrin fluorescence was much weaker for all cells, as previously reported, and the difference between populations was more evident when evaluated relative to chlorophyll than in terms of absolute mean fluorescence values. One must keep in mind that the absolute signal intensities were impacted by the power of the excitation and the gain of the PMT, as well as the efficiency of filters. Thus, the value of the data is in the information it provides on one population relative to the others rather than in the absolute values of the numbers.

IV. CONCLUSIONS

A microflow cytometer was designed to analyze marine algae over a wide size range (at least 1–50 μm) and was equipped with 404 nm and 532 nm lasers in order to maximally excite chlorophyll and phycoerythrin. Four different populations of phytoplankton with a wide range of shapes and fluorescence properties were evaluated. These microorganisms showed different patterns of light scatter and fluorescence signals consistent with variations in size and amounts of intrinsic chlorophyll and phycoerythrin. A more confined core stream decreased the signal variation by limiting the differences in excitation intensity received by each cell. This system is

being adapted for use on unmanned underwater vehicles to track population changes of phytoplankton over time.[22]

ACKNOWLEDGMENTS

This work was supported by ONR/NRL 6.2 work unit 69-6339. Nastaran Hashemi is an American Society for Engineering Education (ASEE) Postdoctoral Fellow. The authors thank Dr. Alan Weidemann (Naval Research Laboratory, Stennis, MI) and Dr. Lisa Hilliard (National Oceanic and Atmospheric Administration, Charleston, SC) for their assistance with this project. The views expressed here are those of the authors and do not represent opinion or policy of the U.S. Navy or Department of Defense.

[1]G. Beaugrand, P. C. Reid, F. Ibañez, J. Alistair Lindley, and M. Edwards, Science **296**(5573), 1692 (2002); C. Parmesan, Annu. Rev. Ecol. Evol. Syst. **37**(1), 637 (2006).
[2]G. Gerdts and G. Luedke, J. Microbiol. Methods **64**(2), 232 (2006); A. Becker, A. Meister, and C. Wilhelm, Cytometry **48**(1), 45 (2002); Mark A. van Dijk, G. Gregori, H. L. Hoogveld, M. Rijkeboer, M. Denis, A. Malkassian, H. J. Gons, Cytometry, Part A **77A**(10), 911 (2010).
[3]G. B. J. Dubelaar and P. L. Gerritzen, Scientia Marina **64**(2), 255 (2000); M. Thyssen and M. Denis, in *Global Change: Mankind-Marine Environment Interactions*, edited by H.-J. Ceccaldi, I. Dekeyser, M. Girault, and G. Stora (Springer, Netherlands, 2011), p. 293; M. Takabayashi, K. Lew, A. Johnson, A. Marchi, R. Dugdale, and F. P. Wilkerson, J. Plankton Res. **28**(9), 831 (2006).
[4]S. Shoji, K. Akahori, K. Tashiro, H. Sato, and N. Honda, RIKEN Rev. **36**, 8 (2001).
[5]A. Wolff, I. R. Perch-Nielsen, U. D. Larsen, P. Friis, G. Goranovic, C. R. Poulsen, J. P. Kutter, and P. Telleman, Lab Chip **3**(1), 22 (2003).
[6]N. Sundararajan, M. S. Pio, L. P. Lee, A. A. Berlin, J. Microelectromech. Syst. **13**(4), 559 (2004).
[7]H. Sato, Y. Sasamoto, D. Yagyu, T. Sekiguchi, and S. Shoji, J. Micromech. Microeng. **17**(11), 2211 (2007).
[8]X. Mao, J. R. Waldeisen, and T. J. Huang, Lab Chip **7**(10), 1260 (2007).
[9]G. Hairer and M. Vellekoop, Microfluid. Nanofluid. **7**(5), 647 (2009).
[10]N. Hashemi, J. S. Erickson, J. P. Golden, K. M. Jacksona, and F. S. Ligler, Biosens. Bioelectron **26**(11), 4263 (2011).
[11]N. Hashemi, P. B. Howell, Jr., J. S. Erickson, J. P. Golden, and F. S. Ligler, Lab Chip **10**(15), 1952 (2010).
[12]P. B. Howell, Jr., J. P. Golden, L. R. Hilliard, J. S. Erickson, D. R. Mott, and F. S. Ligler, Lab Chip **8**(7), 1097 (2008).
[13]J. P. Golden, J. S. Kim, J. S. Erickson, L. R. Hilliard, P. B. Howell, G. P. Anderson, M. Nasir, and F. S. Ligler, Lab Chip **9**(13), 1942 (2009).
[14]C. S. Yentsch and C. M. Yentsch, J. Marine Res. **37**(3), 471 (1979); R. J. Olson, D. Vaulot, and S. W. Chisholm, Deep Sea Res., Part A **32**(10), 1273 (1985).
[15]C. S. Yentsch, B. E. Lapointe, N. Poulton, and D. A. Phinney, Harmful Algae **7**(6), 817 (2008).
[16]J. B. Waterbury, S. W. Watson, R. R. L. Guillard, L. E. Brand, Nature **277**(5694), 293 (1979).
[17]S. W. Jeffrey, M. Sielicki, and F. T. Haxo, J. Phycol. **11**(4), 374 (1975).
[18]D. A. Phinney and T. L. Cucci, Cytometry **10**(5), 511 (1989).
[19]A. Amato, L. Orsini, D. D'Alelio, and M. Montresor, J. Phycol. **41**(3), 542 (2005); L. J. Ong and A. N. Glazer, J. Biol. Chem. **262**(13), 6323 (1987); T. Gillbro and R. J. Cogdell, Chem. Phys. Lett. **158**(3–4), 312 (1989).
[20]S. M. Davison and K. V. Sharp, in *Proceedings of the COMSOL Multiphysics Users' Conference* (2006).
[21]B. R. Watts, T. Kowpak, Z. Zhang, C.-Q. Xu, and S. Zhu, Biomed. Opt. Express **1**(3), 848 (2010).
[22]G. B. J. Dubelaar, P. J. F. Geerders, and R. R. Jonker, J. Environ. Monit. **6**(12), 946 (2004).